The Astrophysical Journal, 798:33 (5pp), 2015 January 1 doi:10.1088/0004-637X/798/1/33

EMPIRICAL DETERMINATION OF EINSTEIN *A*-COEFFICIENT RATIOS OF BRIGHT [Fe II] LINES*

T. Giannini[1], S. Antoniucci[1], B. Nisini[1], D. Lorenzetti[1], J. M. Alcalá[2], F. Bacciotti[3], R. Bonito[4,5], L. Podio[3], and B. Stelzer[4]
[1] INAF-Osservatorio Astronomico di Roma, Via Frascati 33, I-00040 Monte Porzio Catone, Italy; teresa.giannini@oa-roma.inaf.it
[2] INAF-Osservatorio Astronomico di Capodimonte, Via Moiariello 16, I-80131 Napoli, Italy
[3] INAF-Osservatorio Astrofisico di Arcetri, Largo E. Fermi 5, I-50125 Firenze, Italy
[4] INAF-Osservatorio Astronomico di Palermo, Piazza del Parlamento 1, I-90134 Palermo, Italy
[5] Dipartimento di Fisica e Chimica, Universitá di Palermo, Piazza del Parlamento 1, I-90134 Palermo, Italy
Received 2014 July 3; accepted 2014 October 24; published 2014 December 18

ABSTRACT

The Einstein spontaneous rates (*A*-coefficients) of Fe^+ lines have been computed by several authors with results that differ from each other by up to 40%. Consequently, models for line emissivities suffer from uncertainties that in turn affect the determination of the physical conditions at the base of line excitation. We provide an empirical determination of the *A*-coefficient ratios of bright [Fe II] lines that would represent both a valid benchmark for theoretical computations and a reference for the physical interpretation of the observed lines. With the ESO–Very Large Telescope X-shooter instrument between 3000 Å and 24700 Å, we obtained a spectrum of the bright Herbig–Haro object HH 1. We detect around 100 [Fe II] lines, some of which with a signal-to-noise ratios $\geqslant$100. Among these latter lines, we selected those emitted by the same level, whose dereddened intensity ratios are direct functions of the Einstein *A*-coefficient ratios. From the same X-shooter spectrum, we got an accurate estimate of the extinction toward HH 1 through intensity ratios of atomic species, H I recombination lines and H_2 ro-vibrational transitions. We provide seven reliable *A*-coefficient ratios between bright [Fe II] lines, which are compared with the literature determinations. In particular, the *A*-coefficient ratios involving the brightest near-infrared lines (λ12570/λ16440 and λ13209/λ16440) are in better agreement with the predictions by the Quinet et al. relativistic Hartree–Fock model. However, none of the theoretical models predict *A*-coefficient ratios in agreement with *all* of our determinations. We also show that literature data of near-infrared intensity ratios better agree with our determinations than with theoretical expectations.

Key words: atomic data – Herbig–Haro objects – ISM: atoms – ISM: individual objects (HH1) – ISM: lines and bands

1. INTRODUCTION

Spectra of nebular environments are commonly characterized by forbidden atomic lines in emission. Usually, the brightest lines are those coming from the fine structure, ground-state levels of the most abundant species, such as oxygen, nitrogen, and sulfur. Although bright, these lines are few in number and sensitive to specific excitation conditions, being, therefore, unable to trace gradients in the physical parameters inside the gas (e.g., Bacciotti & Eislöffel 1999; Giannini et al. 2013). Moreover, diagnostic tools based on flux ratios between lines of different species require one to assume the relative elemental abundances, which in turn imply an uncertainty on the derived physical parameters that can exceed 40% (Podio et al. 2006). All of these limitations can be circumvented by using flux ratios of lines from the same species, which cover a wide range of excitation conditions and are also valuable to probe the extinction value. In this sense, UV to near-infrared (NIR) [Fe II] lines, have recently been proven as being very powerful diagnostic tools (Giannini et al. 2013). The main limitation of iron diagnostics is derived from the computational method adopted to describe the quite complex atomic system of iron, from which the derivation of atomic parameters (both radiative and collisional) depends. By combining the uncertainties on *A*-coefficients, collisional coefficients, and their propagation on the level populations, Bautista et al. (2013) have shown that the uncertainties on the line emissivity can be larger than 60%. These uncertainties imply a poor determination of the physical parameters: for example a difference of 30% in the *A*-coefficients in the [Fe II]λ12570/λ16440 flux ratio, which is commonly used to estimate the reddening, gives an uncertainty on A_V of about 3 mag.

In addition to a number of theoretical efforts (Nussbaumer & Storey 1988; Quinet et al. 1996; Deb & Hibbert 2011, hereafter DB), an attempt to empirically derive the rates for spontaneous emission of bright [Fe II] lines, has been done by Smith & Hartigan (2006) by means of observations on the P Cygni's nebula. This method, originally proposed by Gredel (1994), considers that the intensity ratio of optically thin lines coming from the same upper level does not depend on the level population (and hence on temperature and density of the emitting gas and/or source variability), but rather is simply $I_{ij}/I_{ik} = A_{ij}\nu_{ij}/A_{ik}\nu_{ik}$, where A_{ij}, A_{ik} and ν_{ij}, ν_{ik} are the Einstein *A*-coefficients and the frequencies of the $i \rightarrow j$, $i \rightarrow k$ lines emitted by the i level. This observational approach has the definite advantage of providing a direct measure of the *A*-coefficient ratios, but it can be applied only if the extinction for which the observed line intensities are de-reddened is known with great accuracy. In the case of P Cygni's nebula, the assumed extinction ($A_V = 1.89$; Lamers et al. 1983) gives, for example, an intrinsic λ12570/λ16440 *A*-coefficient ratio of 1.13, which is definitively higher than all of the theoretical computations

* Based on observations collected with X-shooter at the Very Large Telescope on Cerro Paranal (Chile), operated by the European Southern Observatory (ESO). Program ID: 092.C-0058(A).

Table 1
Fluxes of Bright [Fe II] Lines

λ_{vac} (Å)	Term Lower–Upper	$F \pm \Delta F$ (10^{-15} erg s^{-1} cm^{-2})
4289	$a^6D_{9/2}$–$a^6S_{5/2}$	0.386 ± 0.002
4360	$a^6D_{7/2}$–$a^6S_{5/2}$	0.294 ± 0.002
7174	$a^4F_{7/2}$–$a^2G_{7/2}$	0.320 ± 0.001
7390	$a^4F_{5/2}$–$a^2G_{7/2}$	0.247 ± 0.001
7639	$a^6D_{7/2}$–$a^4P_{5/2}$	0.276 ± 0.001
8619	$a^4F_{9/2}$–$a^4P_{5/2}$	2.605 ± 0.002
12570	$a^6D_{9/2}$–$a^4D_{7/2}$	26.56 ± 0.005
13209	$a^6D_{7/2}$–$a^4D_{7/2}$	7.461 ± 0.002
15339	$a^4F_{9/2}$–$a^4D_{5/2}$	2.63 ± 0.02
15999	$a^4F_{7/2}$–$a^4D_{3/2}$	1.57 ± 0.015
16440	$a^4F_{9/2}$–$a^4D_{7/2}$	23.93 ± 0.030
16773	$a^4F_{7/2}$–$a^4D_{5/2}$	2.11 ± 0.02
17116	$a^4F_{5/2}$–$a^4D_{3/2}$	0.433 ± 0.002

provided in the literature (roughly ranging between 0.79 and 1.04). In a previous work (Giannini et al. 2008), we compared this value (together with all of the other available in the literature at that time) with a number of observations, but we did not find a consistency between observational data and theoretical or empirically derived predictions.

In the present work, we want to revisit this issue and derive some [Fe II] A-coefficient ratios by means of observations specifically planned to this aim. We targeted a well-known and very bright object, namely, the bow-show at the edge of the HH 1 protostellar jet (Raga et al. 2011 and references therein, hereinafter HH 1). This source is extremely rich in emission lines from different species covering a wide spectral range from the UV to the NIR (Solf et al. 1988; T. Giannini et al. 2015, in preparation), which allow one to derive a precise estimate of the reddening by means of several independent tracers. The target was observed exploiting the unique capabilities of sensitivity and simultaneous spectral coverage of the X-shooter spectrograph at the ESO Very Large Telescope (VLT), circumstances that allow us both to get an exceptionally high signal-to-noise ratio (S/N) on the bright lines and to partially overcome possible intercalibration problems among different spectral segments.

The paper is organized as follows. In Section 2, we present the X-shooter observations and the data reduction. In Section 3.1 independent A_V determinations are provided, while, in Sections 3.2 and 3.3, we comment on the A-coefficient ratios obtained for bright and valuable diagnostic Fe^+ lines. A summary is then given in Section 4.

2. OBSERVATIONS AND DATA REDUCTION

We collected seven X-shooter (Vernet et al. 2011) observations of HH 1 ($\alpha_{J2000.0} = 05^h36^m20\overset{s}{.}27$, $\delta_{J2000.0} = -06°45'04\overset{''}{.}84$, distance of 414 pc), in the period of 2013 November 1–2014 January 2, each integrated by about 30 minutes on-source. Since the object ($9'' \times 12''$) fills the $11''$ slit along the spatial direction, sky observations were performed with dedicated exposures taken around $10''$ apart from the scientific target and integrated by as much time as on-source. The slit, aligned with the direction of the bow-shock (position angle of 129°), was set to achieve a resolution power of 9900, 18,200, and 7780 for the UVB (3000–5900 Å), VIS (5450–10200 Å), and NIR arm (9900–24700 Å), respectively (slit widths: $0\overset{''}{.}5$, $0\overset{''}{.}4$, $0\overset{''}{.}6$). The pixel scale is $0\overset{''}{.}16$ for the UVB and VIS arm, and $0\overset{''}{.}21$ for the NIR arm. The data reduction was accomplished independently for each arm using the X-shooter pipeline v.2.2.0 (Modigliani et al. 2010), which provides two-dimensional spectra, both flux and wavelength calibrated. Post-pipeline procedures were then applied by using routines within the IRAF package to subtract the sky-exposures, correct the observed radial velocities for all the motions of the Earth with respect to the direction of the target, combine the seven observations (after having verified that in the single exposures none of the brightest [Fe II] lines is contaminated by telluric features), and extract the final one-dimensional spectra. In addition, each NIR image was divided by the spectrum of a telluric standard star taken immediately after the target observation, which was corrected for both the stellar continuum shape and the intrinsic absorption features (hydrogen recombination lines). The goodness of the intercalibration between adjacent arms was checked by comparing fluxes of lines present in the overlapping portions of the spectrum, since this lacks a bright continuum emission. While several lines are present in both the UVB and VIS spectra, with fluxes that agree within a few percent, only one line (H I λ10048) is detected in both the VIS and NIR arm, because the NIR flux is about 40% higher. We applied this intercalibration factor to the NIR spectrum to realign it with the other two segments. However, to minimize any possible source of uncertainty, we have avoided determining A-coefficient ratios of [Fe II] lines lying in different arms. Also, to derive the extinction value (Section 3), we preferentially used the ratios of lines lying in the same arm or in the UVB or VIS arms.

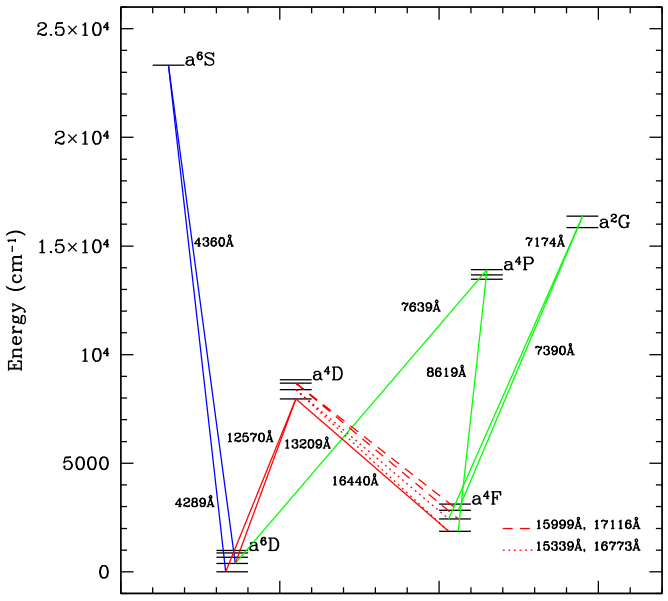

Figure 1. Grotrian diagram of [Fe II] with the lines discussed in this paper. UVB, VIS, and NIR lines are depicted in blue, green, and red, respectively.

3. RESULTS AND ANALYSIS

The HH 1 spectrum results in exceptionally rich emission lines, with more than 500 detections of fine structure atomic lines, hydrogen and helium recombination lines, and H_2 rovibrational lines (T. Giannini et al. 2014, in preparation); in particular, around 100 lines come from [Fe II] transitions. Those used in this paper to derive the A-coefficient ratios all have S/Ns $\gtrsim$ 100 (see Table 1 and Figure 1). The line fluxes are computed by integrating the emission below the line profile,

Table 2
Comparison of *A*-coefficient Ratios of Bright [Fe II] Lines

Ratio	NS	Q-SST	Q-HFR	DB	SH	This Work	
			A-coefficient Ratios			*A*-coefficient Ratios	Intrinsic Intensity Ratios[a]
λ12570/λ16440	1.04	0.79	0.90	1.04	1.13	0.84–0.92	1.11–1.20
λ13209/λ16440	0.29	0.22	0.24	0.29	0.32	0.25–0.27	0.31–0.33
λ15339/λ16773	1.26	1.25	1.26	1.25	1.07	1.12–1.18	1.22–1.27
λ15995/λ17116	3.56	3.54	3.57	3.55	3.05	3.20–3.59	3.43–3.84
λ7639/λ8619	0.13	0.19	0.23	0.43	···	0.09–0.10	0.10–0.12
λ7174/λ7390	···	1.31	1.31	1.31	···	1.25–1.30	1.29–1.34
λ4289/λ4360	···	1.34	1.35	···	···	1.25–1.32	1.27–1.34

Notes. [a] Intrinsic intensity ratios, computed multiplying the derived *A*-coefficient ratios times the vacuum frequencies ratios, taken from the "The atomic line list, v2.04" (http://www.pa.uky.edu/~peter/atomic/).
References. NS: Nussbaumer & Storey (1988); Q-SST: Quinet et al. (1996)—SuperStructure; Q-HFR: Quinet et al. (1996)—relativistic Hartree–Fock; DB: Deb & Hibbert (2011); SH: Smith & Hartigan (2006).

while the errors are obtained by multiplying the noise (rms) at the line base times the FWHM of the line profile.

3.1. A_V Determination

As anticipated in Section 1, a reliable observational estimate of the Einstein *A*-coefficient ratios can be obtained only provided that the extinction toward the target is determined with a very good accuracy. A powerful way to achieve this is to use pairs of optically thin transitions for which the atomic parameters are accurately known and that come from the same upper level, since in this case the difference between the observed and the theoretical flux ratio is a function only of the extinction amount. In the case of HH 1, thanks to the rather large number of bright lines detected in the spectrum, independent extinction estimates can be derived from a number of line ratios. We consider hydrogen recombination lines, atomic fine structure lines, and H_2 ro-vibrational lines. The atomic data (*A*-coefficients and vacuum frequencies) are taken from "The atomic line list," v2.04,[6] and from the "National Institute of Standards and Technology" database[7], while H_2 frequencies and *A*-coefficients are from Dabrowski (1984) and Wolniewicz et al. (1998), respectively. To minimize the uncertainties, we consider ratios of unblended lines detected with an S/N > 30.

Ratios of H I lines coming from the same upper level involve different series, which in our case are the Balmer, Paschen, and Brackett series. Given the optimal alignment between the UVB and VIS arms, we have considered only ratios of unblended lines of the Balmer and Paschen series in these two arms (i.e., Balmer lines with $n_{up} \geqslant 4$ and Paschen lines with $n_{up} \geqslant 7$), with the exception of a few ratios involving very bright NIR lines (namely, Paδ/H7; Paγ/Hδ; Paβ/Hγ; Brγ/Paδ). Lines that appear contaminated by artifacts or sky line residuals in the spectral images are also discarded. In Figure 2, we plot the Balmer and Paschen decrements (upper and middle panels) as a function of the upper quantum number. Their distribution is well fitted with a case B (Hummer & Storey 1987) distribution at $3000 \leqslant T \leqslant 20{,}000$ K and low density ($n = 10^4$ cm^{-3}), which ensures that the lines are optically thin. To estimate the extinction, we apply the reddening law of Cardelli et al. (1989), after having checked that very marginal differences are found if the Rieke & Lebofsky (1985) or the Weingartner & Draine (2001) laws are applied. Similarly, the possible effect of a patchy extinction, which should provide a change in the extinction law, is likely negligible. If this were the case, indeed, lines at shorter wavelengths would be more opaque, and therefore a weak trend of the green points being further above the red ones (as n_{up} increases) should be recognizable. Also, the ratio of total to selective extinction (R_V) was assumed to vary between three and five.

The A_V estimate was obtained by averaging each independent determination (12 lines ratios). We get $A_V = 0.3 \pm 0.1$ mag and $A_V = 0.6 \pm 0.2$ mag, for $R_V = 3$ and $R_V = 5$, respectively. For example, in the bottom panel of Figure 2 we plot the observed (black) and the theoretical ratios (red) along with the observed ratios (green) de-reddened for $A_V = 0.3 \pm 0.1$ mag, $R_V = 3$.

Lower A_V values are derived from line ratios of fine structure lines. In particular, we use ratios of [Ni II] (λ4629/λ7258 and λ7380/λ19393), [S II] (λ4070/λ10289 and λ4077/λ10339), and [S III] (λ9071/λ9533), which on average give $A_V = 0.15 \pm 0.15$ mag for $R_V = 3$ ($A_V = 0.30 \pm 0.15$ mag for $R_V = 5$). Finally, ratios of H_2 ro-vibrational lines (2-0Q(*i*+2)/2-0O(*i*), with *i* between 1 and 4), give $A_V \sim 0$ mag. These three determinations, though similar to each other, may indicate that lines from different species likely originate in different areas within the shock, where extinction undergoes a small gradient. Since we are unable to determine from which of these areas [Fe II] lines originate, we assume a range of A_V from 0.0 mag to a conservative value of 0.8 mag.

3.2. *A*-coefficient Ratios of [Fe II] Lines

In Table 2, we report the theoretical estimates of seven *A*-coefficient ratios derived by different authors under different approximations for the Fe^+ atomic model (see caption of Table 2 for references) and the observational determination by Smith & Hartigan (2006, hereafter SH). In the seventh column we give the *A*-coefficient ratios derived in the present work. These are presented as a range of values, obtained by combining as uncertainties both the flux errors of Table 1 and the two extreme extinction estimates of 0.0 mag and 0.8 mag derived in Section 3.1. The last column reports the intrinsic intensity ratios computed on the base of the derived *A*-coefficient ratios. Notably, none of the literature determinations are in agreement with *all* of our values. In particular, for λ12570/λ16440 and λ13209/λ16440 *A*-coefficient ratios, we find values close to the Q-HFR predictions, while our determination for λ15339/λ16773 is in between the theoretical predictions and the SH empirical derivation. A large spread is found between theoretical predictions for λ7639/λ8619, which are, however, all above our derived range. Finally, we find a marginal agreement with

[6] http://www.pa.uky.edu/~peter/atomic/
[7] http://www.nist.gov/pml/data/asd.cfm

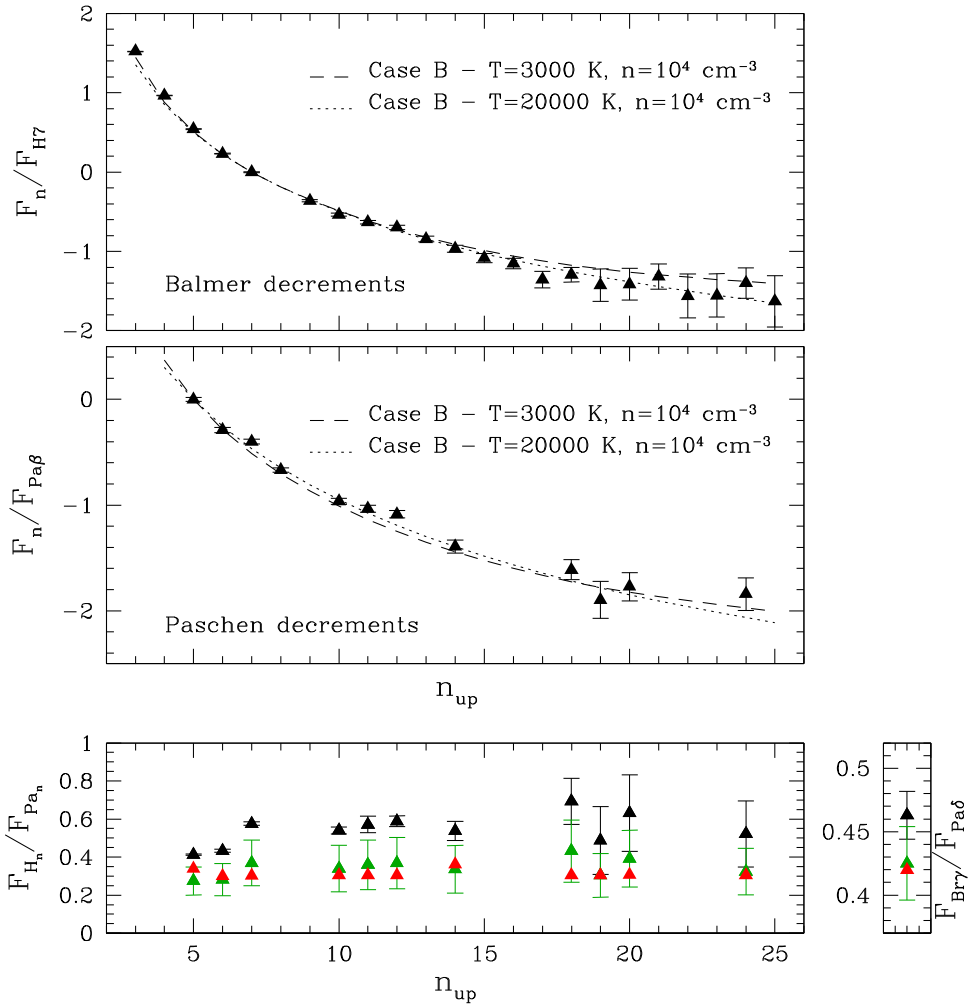

Figure 2. Top and middle panels: Balmer and Paschen observed decrements fitted with case B recombination models. The best fits correspond to $n = 10^4$ cm^{-3} and $3000 \leqslant T \leqslant 20{,}000$ K, obtained by normalizing the Paschen decrements to the Pβ and the Balmer decrements to the H7. In both panels, we plot only the lines that are not blended with lines from other species and not contaminated by artifacts or sky line residuals in the spectral images. Bottom panel (left): ratios of Balmer and Paschen lines coming from the same upper level. Black symbols are the observed ratios, red symbols are the theoretical values, and green symbols are the observed ratios once dereddened for $A_V = 0.2$–0.4 mag (estimated for $R_V = 3$). Bottom panel (right): same as in the left panel for the Brγ/Paδ ratio.

the Q-SST, Q-HFR, and DB determinations for λ7174/λ7390 and λ4289/λ4360 *A*-coefficient ratios, while our range for λ15995/λ17116 is in agreement with all the theoretical models and keeps out only the SH determination.

3.3. Comparison with Observations

The intrinsic intensity ratios of the first two pairs of lines, namely, $I(\lambda 12570)/I(\lambda 16440)$ and $I(\lambda 13209)/I(\lambda 16440)$, are of great interest since they involve lines commonly observed in the spectra of nebular environments that are often used to derive the extinction toward the target. In a previous work (Giannini et al. 2008, Figure 5), we have already shown how the theoretical intensity ratios are unable to fit the observations of a number of Herbig–Haro (HH) objects where these lines were observed with a high S/N. Here we reproduce the same figure (Figure 3) but including both new observational determinations and up-to-date theoretical determinations. These are depicted as black curves that start at the expected value for $A_V = 0$ mag and then follow the reddening law of Cardelli et al. (1989) up to $A_V \sim 20$ mag. Notably, no appreciable differences are found if other extinction laws are adopted (e.g., Rieke & Lebofsky 1985) also given the short wavelength range taken into consideration. The same reddening law is depicted in red for the starting points (those for $A_V = 0$ mag) derived in this work, and the open and filled circles are the points corresponding to an A_V toward HH 1 of 0.0 and 0.8 mag, respectively. By examining the plot, several conclusions can be drawn. (1) All of the theoretically derived intrinsic intensity ratios are not consistent with the large majority of the data points, irrespective of the extinction values. (2) The SH curve roughly superposes that derived in the present work, though starting from a different $A_V = 0$ mag point. This result reinforces the goodness of the empirical approach adopted both in the SH and in the present work, but, on the other hand, it provides evidence that the empirical method is powerful only provided that the extinction toward the target is accurately known. In particular, we hypothesize that the extinction value (∼2 mag) for which the P Cygni data points have been de-reddened is too high. Indeed, if the SH intrinsic ratio were assumed ($I(\lambda 13209)/I(\lambda 16440) = 0.39$; $I(\lambda 12570)/I(\lambda 16440) = 1.49$) the extinction toward HH 1 would be around 2–3 mag, i.e., not in agreement with our estimates. (3) Despite the overall better agreement of our predictions with the observational data, a significant number of points, and in particular those associated with low extinction values, tend to remain to the right of our theoretical curve. Although small (e.g., a decrease of less than 10% of $I(\lambda 13209)/I(\lambda 16440)$

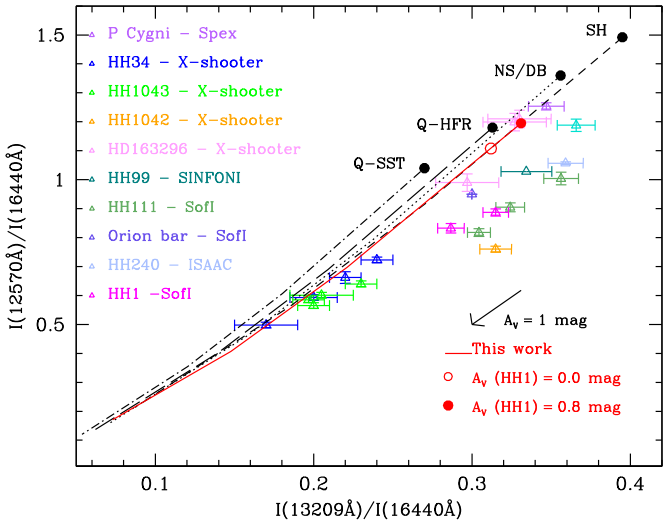

Figure 3. $I(12570\ \text{Å})/I(16440\ \text{Å})$ vs. $I(13209\ \text{Å})/I(16440\ \text{Å})$ measured in bright objects (depicted with different colors, note that some objects have several data points, corresponding to different knots of emission). Intrinsic line ratios theoretically predicted (Q-SST: Quinet et al. 1996—SuperStructure; Q-HFR: Quinet et al. 1996—relativistic Hartree–Fock; NS: Nussbaumer & Storey 1988; DB: Deb & Hibbert 2011), along with the empirical point by Smith & Hartigan (2006, SH) are labeled. The black curves represent the extinction law by Cardelli et al. (1989), applied to the theoretical points; in red is shown the same curve derived in the present work, which starts from the open or filled circle if A_V toward HH 1 is 0.0 or 0.8 mag. The extinction vector corresponding to $A_V = 1$ mag is depicted as well. Data from literature: HH111, HH240: Nisini et al. (2002); HH1: Nisini et al. (2005); P Cygni: Smith & Hartigan (2006); HH99: Giannini et al. (2008); Orion bar: Walmsley et al. (2000); HH34: B. Nisini et al. (2015, in preparation); HH1042, HH1043: Ellerbroek et al. (2013); HD 163296: Ellerbroek et al. (2014).

would be sufficient to shift the observed data on our theoretical curve), such an effect appears to by systematic, and therefore deserves a deeper investigation, in particular, as far as possible instrumental effects are concerned. In this respect, first we note that, at intermediate spectral resolutions, three telluric features at $\lambda_{\rm air} = 13207.3$ Å, 16437.7 Å, and 16443.1 Å (Oliva & Origlia 1992) may shift into or away from the [Fe II] lines depending on the terrestrial motion around the Sun at the time of the observation. More importantly, these telluric features blend fully with the [Fe II] lines if the spectral resolution is less than a few thousands. Second, flux intercalibration between different spectral segments may have a role, especially for long-lasting observations during which the atmospheric conditions may highly change. Indeed, in Figure 3, the largest deviations are associated with low-resolution data taken with spectrographs, such as SofI at ESO–New Technology Telescope or ISAAC at ESO–VLT, which do not cover the three line wavelengths simultaneously. Conversely, the X-shooter observations, which are taken in one shot and with R larger than 10000, are more consistent with our theoretical curve (although with few exceptions, e.g., HH 1042).

4. SUMMARY

We have exploited the exceptionally bright X-shooter spectrum of the Herbig–Haro object HH 1 to observationally derive Einstein A-coefficient ratios of bright [Fe II] lines commonly observed in the spectra of nebular environments. These were derived from the observed intensity ratios of lines emitted from the same level, once properly de-reddened for the extinction toward the target. This was accurately determined by means of independent tracers, namely, hydrogen recombination lines, atomic fine structure lines and H_2 ro-vibrational lines. We are able to give a meaningful range of A-coefficient ratios for seven pairs of [Fe II] lines, which have been compared with the theoretical determinations available in the literature. Notably, none of the latter are consistent with *all* of our determinations. The comparison of the intrinsic $\lambda12570/\lambda16440$ and $\lambda13209/\lambda16440$ intensity ratios derived in this work, and a number of observations, shows that our determinations better agree with a large set of observations, though a significant number of literature data still lies to the right of the reddening line. Further observations are required to determine if such discrepancy is due to instrumental effects, as we hypothesize.

In conclusion, although our analysis is limited to a few bright lines, it represents a valuable effort to *observationally* solve the problem of the determination of the A-coefficient ratios of [Fe II] lines. These new determinations, which involve lines commonly observed in nebular environments, will be of great help in tracing the physical conditions (temperature, density, extinction) of the emitting gas.

We kindly thank A. Hibbert for providing the Deb & Hibbert (2011) list of A-coefficients of Fe^+ lines. The ESO staff is acknowledged for support with the observations and the X-shooter pipeline. Financial support from INAF, under PRIN2013 program "Disks, jets and the dawn of planets" is also acknowledged.

REFERENCES

Bacciotti, F., & Eislöffel, J. 1999, A&A, 342, 717
Bautista, M. A., Fivet, V., Quinet, P., et al. 2013, ApJ, 770, 15
Cardelli, J. A., Clayton, G. C., & Mathis, J. S. 1989, ApJ, 345, 245
Dabrowski, I. 1984, CaJPh, 62, 1634
Deb, N. C., & Hibbert, A. 2011, A&A, 536, A74
Ellerbroek, L. E., Bik, A., Kaper, L., et al. 2013, A&A, 558, A102
Ellerbroek, L. E., Podio, L., Dougados, C., et al. 2014, A&A, 563, A87
Giannini, T., Calzoletti, L., Nisini, B., et al. 2008, A&A, 481, 123
Giannini, T., Nisini, B., Antoniucci, S., et al. 2013, ApJ, 778, 71
Gredel, R. 1994, A&A, 292, 580
Hummer, D. G., & Storey, P. J. 1987, MNRAS, 224, 801
Lamers, H. J. G. L. M., de Groot, M., & Cassatella, A. 1983, A&A, 128, 299
Modigliani, A., Goldoni, P., Royer, F., et al. 2010, Proc. SPIE, 7737, 773728
Nisini, B., Bacciotti, F., Giannini, T., et al. 2005, A&A, 441, 159
Nisini, B., Caratti o Garatti, A., Giannini, T., & Lorenzetti, D. 2002, A&A, 393, 1035
Nussbaumer, H., & Storey, P. J. 1988, A&A, 193, 327
Oliva, E., & Origlia, L. 1992, A&A, 254, 466
Podio, L., Bacciotti, F., Nisini, B., et al. 2006, A&A, 456, 189
Quinet, P., Le Dourneuf, M., & Zeippen, C. J. 1996, A&AS, 120, 361
Raga, A. C., Reipurth, B., Cantó, J., Sierra-Flores, M. M., & Guzmán, M. V. 2011, RMxAA, 47, 425
Rieke, G. H., & Lebofsky, M. J. 1985, ApJ, 288, 618
Smith, N., & Hartigan, P. 2006, ApJ, 638, 1045
Solf, J., Bohm, K. H., & Raga, A. 1988, ApJ, 334, 229
Vernet, J., Dekker, H., D'Odorico, S., et al. 2011, A&A, 536, A105
Walmsley, C. M., Natta, A., Oliva, E., & Testi, L. 2000, A&A, 364, 301
Weingartner, J. C., & Draine, B. T. 2001, ApJ, 548, 296
Wolniewicz, L., Simbotin, I., & Dalgarno, A. 1998, ApJS, 115, 293